Original Article

Effect of Yttrium Oxide Nanoparticles on Liver Fibrosis Induced by Carbon Tetrachloride in Male Rats

Fatemeh Danesh Pajooh[1], PhD candidate;
Shahrbanoo Oryan[1,2], PhD;
Pejman Mortazavi[3], PhD

[1]Department of Biology, Science and Research Branch, Islamic Azad University, Tehran, Iran;
[2]Department of Animal Sciences, Faculty of Biological Sciences, Kharazmi University, Tehran, Iran;
[3]Department of Pathology, School of Specialized Veterinary Sciences, Science and Research Branch, Islamic Azad University, Tehran, Iran

Correspondence:
Shahrbanoo Oryan, PhD;
Department of Animal Sciences, School of Biological Sciences, Kharazmi University, No. 43, South Mofatteh Ave., Postal Code: 15719-14911, Tehran, Iran
Tel: +98 26 34579600
Email: drshahrbanooryan@gmail.com
Received: 04 November 2025
Revised: 23 February 2026
Accepted: 13 March 2026

Abstract

Background: Yttrium oxide nanoparticles (Y_2O_3 NPs) are known as free radical absorbers. This study investigated the effects of Y_2O_3 NPs on antioxidant activities, liver enzymes, expression of alpha-smooth muscle actin (*α-SMA*) and transforming growth factor beta (*TGF-β*) genes, and histopathology in rat liver fibrosis.

Methods: In this experimental study conducted in 2019 at Islamic Azad University, Qom, Iran, male Wistar rats (200–220 g) were assigned to seven groups (n=8): Control, Vehicle, carbon tetrachloride (CCl_4), Y_2O_3 45 mg/Kg, Y_2O_3 60 mg/Kg, CCl_4+Y_2O_3 45 mg/Kg, and CCl_4+Y_2O_3 60 mg/Kg. Liver fibrosis was induced by CCl_4. Y_2O_3 NPs were administered intraperitoneally for 4 weeks. Blood and liver samples were collected for analyses. Statistical analysis was performed using SPSS (version 21) by one-way ANOVA and Tukey *post hoc* test. $P<0.05$ was considered significant.

Results: The findings indicated catalas (3.00±0.21 vs. 21.46±0.70, 8.96±20 U/min/mg, $P<0.001$), superoxide dismutase (3.13±0.21 vs. 44.36±1.99, 37.59±0.77 U/mg, $P<0.001$), glutathione peroxidase (135.25±4.02 vs. 492.00±27.87, 322.75±8.75, U/mg, $P<0.001$) activities increased, while malondialdehyde (1.29±0.86 vs. 0.32±0.03 , 0.49±0.06 nmol/mL, $P<0.001$), aspartate aminotransferase (286.33±2.89 vs. 154.66±9.00, 178.00±7.35 U/L, $P<0.001$), alkaline phosphatase (645.00±16.62 vs. 497.66±9.87, 321.75±20.03 U/L, $P<0.001$), gamma-glutamyl transferase (619.00±23.45 vs. 349.66±29.95, 299.25±2541 U/L, $P<0.001$) levels decreased. TGF-β and α-SMA expression decreased in terated groups (6.40±0.23 to 4.19±0.55, $P=0.012$, 2.70±0.46 $P=0.009$, 13.77 ±0.44 to 7.94±0.54 $P=0.002$, 4.87±0.35 $P=0.033$). Histology evaluatuons confirmed reduced inflammation, steatosis, and collagen deposition in Y_2O_3-treated fibrotic rats.

Conclusion: Y_2O_3 NPs can alleviate liver fibrosis in experiment.

Please cite this article as: Danesh Pajooh F, Oryan S, Mortazavi P. Effect of Yttrium Oxide Nanoparticles on Liver Fibrosis Induced by Carbon Tetrachloride in Male Rats. Iran J Med Sci. doi: 10.30476/ijms.2026.109288.4451.

Keywords ● Yttrium oxide nanoparticles ● Liver fibrosis ● Carbon tetrachloride ● Transforming growth factor beta ● Alpha-smooth muscle actin ● Wistar rats

What's Known

- Given the importance of treating liver fibrosis and the spread of nanoparticles in medicine, the use of yttrium oxide nanoparticles (Y_2O_3 NPs) seems appropriate.
- Very few studies have evaluated the therapeutic effects of Y_2O_3 NPs on liver fibrosis induced by CCl_4 in rats.

What's New

- Y_2O_3 NPs alleviated liver fibrosis in this experiment.
- Positive treatment effects of Y_2O_3 NPs in the fibrotic rats induced with CCL_4 are due to increase antioxidant activities, regulation of liver enzymes, *TGF-β* and *α-SMA* genes expression levels.

Introduction

The liver, as a vital organ, has various functions in the body such as detoxification, vitamin storage, digestion, immunity, and help support metabolism.[1] It comprises around 2% of body weight

in the adult.[2] When liver cells are exposed to long-term damage, they cause abnormal cell proliferation and accumulation of tough fibrous connective tissue.[3] The most important factors to the development of liver fibrosis are alcohol, fatty liver, hepatitis B and C and infrequent diseases such as hemochromatosis.[4] Liver fibrosis is a result of a permanent wound-healing response to chronic liver damage[5] and can lead to cirrhosis and liver cancer.[6] Hepatic stellate cell (HSC) activation, hepatocyte cell death, the release of cytokines, chemokine, and inflammation are important causes of liver fibrosis.[7] Fibrosis can be mediated through Smad-dependent or non-Smad pathways.[8] Increased production of transforming growth factor-beta (TGF-β) enhances the expression of alpha-smooth muscle actin (α-SMA) and collagen α1,[9] resulting in the deposition of collagen fibers[10] and contributing to liver fibrosis.[11] The use of traditional therapies, has always had inadequate therapeutic effects and side effects.[12] Recently, the use of nanotechnology for targeted liver therapies has been considered by researchers.[13, 14] By converting microparticles to nanoparticles, some physical properties change,[15] such as increasing the surface area and quantum effects of the particles.[16] Scientists today are able to produce nanoparticles as large as viruses,[17] and according to research, nanoparticles are a more suitable option for intracellular or tissue delivery of drugs.[18] In fact, nanoparticles are good candidates for targeted therapies because they can pinpoint patient cells and deliver the drug to them.[19] This means that the drug can be sufficient at lower doses and therefore fewer side effects.[20] Various studies have suggested the therapeutic effects of yttrium oxide nanoparticles (Y_2O_3 NPs) due to their attractive antioxidant and antibacterial properties.[21]

Measurements levels of oxidative stress markers, such as reactive oxygen species (ROS), lipid peroxidation (LPO), total thiol molecules (TTM), and total anti-oxidant power (TAP) and catalase enzyme in the brain, heart, lung, kidney, liver, and spleen showed that diazinon-induced oxidative stress was reduced in rats treated with Y_2O_3 NPs, but it should be noted that higher doses have the opposite effect.[22] On the other Y_2O_3 NPs improve fulminant hepatic failure through anti-inflammatory activity by inhibiting cellular reactive oxygen species and modulating NF-κB activation.[23] Y_2O_3 NPs can be considered as an important therapeutic option in the treatment of diseases due to its high biocompatibility and reactivity.[24]

Given the importance of treating liver fibrosis and the spread of nanoparticles in medicine, the use of Y_2O_3 NPs seems appropriate. This study was designed to assess the effects of Y_2O_3 NPs on antioxidant enzymes, TGF-β and α-SMA gene expression on liver fibrosis induced by carbon tetrachloride (CCl_4) in rats.

Materials and Methods

Reagents

CCl_4 (Sigma-Aldrich, USA), Y_2O_3 NPs (Ilia Sanat Asan, Iran), catalas (CAT) (Zellbio, Germany), superoxide dismutase (SOD) (Zellbio, Germany), malondialdehyde (MDA) (Zellbio, Germany), glutathione peroxidase (GPX) (Zellbio, Germany), aspartate aminotransferase (AST) (Zist Chem, Iran), alanine aminotransferase(ALT) (Zist Chem, Iran), alkaline phosphatase (ALP) (Zist Chem, Iran), gamma-glutamyl transferase (GGT) (Biorex Fars, Iran), Total RNA extraction Kit (Parstous Zist Fanavar, Iran), cDNA synthesis kits (Parstous Zist Fanavar, Iran), SYBR Green Real-Time polymerase chain reaction (PCR) Master Mixes (Parstous Zist Fanavar, Iran) and, Primers)Pishgam Tehran, Iran) were purchased from the mentioned companies.

Animals

In this experimental animal study, conducted in 2019 at the laboratory of Islamic Azad University, Qom Branch, Qom, Iran, eight to ten week old male Wistar rats, weighing 200 to 220 g (n=8) were obtained from the Pasteur Institute, Tehran, Iran. The animals were housed under standard conditions with temperature of 21 °C under a 12:12 hr light/dark cycle with free access to food and tap water. All animal procedures and care were performed in accordance with the Guide for the Care and Use of Laboratory Animals.[25] The experimental protocol was approved by the Research Ethics Committee of Islamic Azad University, Science and Research Branch, Tehran, Iran (Ethics code: IR.IAU.SRB.REC.1402.203).

Preparation of Y_2O_3 NPs

Yttrium oxide nanoparticles were phosphated before use as follow. Since Y_2O_3 NPs are air-stable white solids and insoluble in water,[26] 10 g of Y_2O_3 NPs were added to 500 mL of tripotassium phosphate (K_3PO_4) at a concentration of 20% and refluxed for 6 hours at 80 °C. The precipitate was separated by a centrifuge (12000 rpm) and dried in a 60 °C oven for 24 hours.[27] Then concentrations of 45 and 60 mg/Kg in saline were prepared for injection.

Rat Model of Liver Fibrosis

In order to induce liver fibrosis, rats received

2 mL/Kg of CCl_4 intraperitoneally (diluted in olive oil, 1:1 ratio) twice a week for 4 weeks.

Experimental Groups

Rats were randomly assigned to seven equal groups using a blocked design (n=7). The control group had access to a normal diet for four weeks. The vehicle group rats that received K3PO4 solution (0.5 mL/Kg, IP) daily for 4 weeks. The CCl_4 group induced liver fibrosis model. The CCl_4+Y_2O_3 groups that received the Y_2O_3 NPs (45 and 60 mg/Kg, IP), respectively, daily for 4 weeks in liver fibrosis model rats. The Y_2O_3 groups that received the Y_2O_3 NPs (45 and 60 mg/Kg, IP), respectively, daily for 4 weeks. Twenty-four hours after last treatment, rats were anesthetized by ketamine 10% and xylasine1%. The blood sample collection from the heart were maintained for 20 min under laboratory conditions and then centrifuged (15 min at 5000 rpm). For the measurement of hepatic enzymes level, serum was collected. The livers were removed later and washed by saline. A slice was kept in 4% formalin for histological analysis. The remained part was frozen at -80 °C for advanced analysis.

Measurement of Oxidative Stress Markers

First, frozen liver tissues were homogenized. Then, they was centrifuged at 40000 rpm for 15 min (4 °C) to separate the supernatant. Oxidative stress markers levels were measured, including CAT, GPX, SOD, and MDA, according to the manufacturer's instructions (Zellbio, Germany) by an Eliza reader.

Liver Enzymes Levels

AST, ALT, and ALP levels were measured using an autoanalyzer (HITACHI 917) according to the manufacturer's instructions (Zist Chem, Iran). GGT enzyme was measured by kit (Biorex Fars, Iran) in agreement with the manufacturer's method.

Liver Real-Time PCR Analysis

YTzol reagent was used in accordance to the kit manufacturer's instructions for total RNA isolation (Parstous Zist Fanavar, Iran). Then quantification procedure was done on the extracted samples by NanoDrop 2000C spectrophotometer (Thermo, United States). Reverse transcription of total RNA to complementary dna (CDNA) was performed using synthesis kit (Parstous Zist Fanavar, Iran). Quantitative real-time PCR (QRT-PCR) reactions were then finalized by SYBR Premix Ex Taq II (Parstous Zist Fanavar, Iran) in the ABI 7500 System. Glyceraldehydes 3-phosphate dehydrogenase (GAPDH) was used (Pishgam Tehran, Iran) as internal control. The specific primer sequences for TGF-β, α-SMA, and GAPDH are presented in table 1. Finally, results were calculated based on the $2^{-\Delta\Delta CT}$ method.

Hematoxylin and Eosin (H&E) and Masson's Trichrome (MTC) Staining

For histopathological examinations, fixed samples were dehydrated and embedded in paraffin. Samples were then cut, mounted on slides, and stained with H&E and MTC methods.[28] The stained slides were studied by an expert pathologist blind to the experiment with a Leica DM500 Biological Microscope.

Statistical Analysis

The results were analyzed using SPSS software (version 22.0, SPSS Inc., Chicago, IL, USA). Data were expressed as mean±standard error of the mean (SEM). Statistical differences between groups were determined by one-way analysis of variance (ANOVA) followed by Tukey's *post hoc* test. A P value of less than 0.05 was considered statistically significant.

Results

Hepatic Analysis of Oxidative Stress

The activities of catalase (CAT), SOD, and glutathione peroxidase (GPX) were markedly altered among the study groups, CAT 251.620, P<0.001; SOD 479.606, P<0.001; GPX 191.871, P<0.001; MDA 20.634, P<0.001). CAT, SOD and GPX activity were substantially decreased in CCl_4 group as compared to control (CAT: 3.00±0.25 vs. 10.05±0.79; SOD: 3.13±0.21 vs. 14.02±0.49; GPX: 135.25±8.06 vs. 281.75±9.18; P<0.001 for all) (figure 1A-C). Administration of Y_2O_3 nanoparticles (45 mg/Kg and 60 mg/Kg) markedly improved antioxidant enzyme activities in fibrotic animals. In the CCl_4+Y_2O_3 45 group,

Table 1: Primers used for the real-time PCR reaction analysis

Gene	Size (bp)	Forward sequence	Reverse sequence
α-SMA	334	GTTTGAGACCTTCAATGTCCC	CGATCTCACGCTCAGCAGTGA
TGF-β	239	GACTCTCCACCTGCAAGACC	GGACTGGCGAGCCTTAGTTT
GAPDH	234	GATGCTGGTGCTGAGTATGTCG	GTGGTGCAGGATGCATTGCTGA

α-SMA: Alpha-smoot muscle actin; TGF-β: Transforming growth factor beta; GAPDH: Glyceraldehyde-3-phosphate dehydrogenase

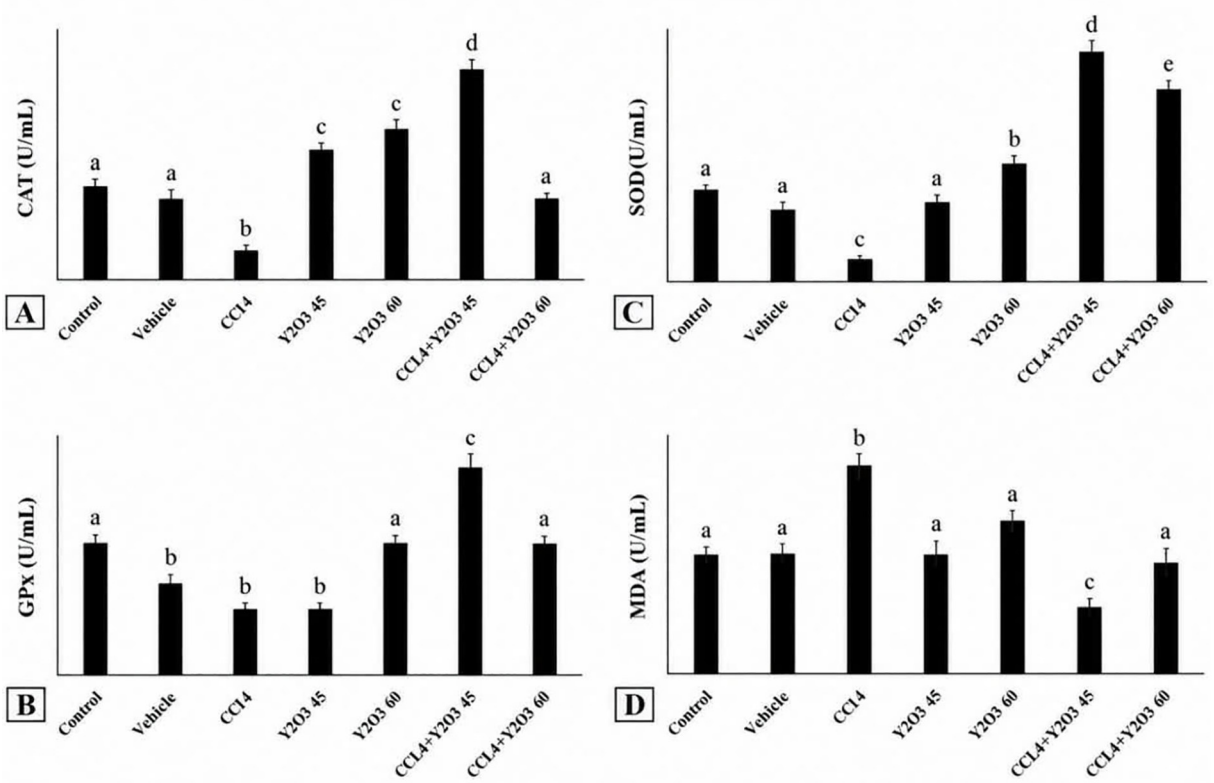

Figure 1: Effects of Y_2O_3 nanoparticles on hepatic oxidative stress markers in different experimental groups. Hepatic oxidative stress markers were assessed. (A) Catalase (CAT) activity, (B) Glutathione peroxidase (GPX) activity, (C) Superoxide dismutase (SOD) activity, and (D) Malondialdehyde (MDA) levels. CCl_4 administration markedly reduced CAT, SOD, and GPX activities and significantly increased MDA levels compared with the Control group (P<0.001), indicating enhanced oxidative stress. Treatment with Y_2O_3 nanoparticles at both 45 and 60 mg/Kg significantly restored antioxidant enzyme activities and reduced lipid peroxidation in fibrotic rats compared with the CCl_4 group (P<0.001). No significant differences were observed between the Control and Vehicle groups in CAT, SOD, or MDA levels.
Control (healthy rats), Vehicle (healthy rats treated with K□PO□), CCl□ (healthy rats treated with CCl□ to induce fibrosis), CCl□+Y□O□45(fibroticratstreatedwith45mg/KgY□O□NPs),CCl□+Y□O□60(fibroticratstreatedwith60mg/KgY□O□NPs),Y□O□45 (healthy rats treated with 45 mg/Kg Y□O□ NPs), Y□O□ 60 (healthy rats treated with 60 mg/Kg Y□O□ NPs).
CAT: Catalase; GPX: Glutathione peroxidase; SOD: Superoxide dismutase; MDA: Malondialdehyde; Y_2O_3 NPs: Yttrium oxide nanoparticles; CCl_4: Carbon tetrachloride; K_3PO_4: Potassium phosphate.

the values increased to (CAT 21.46±1.00, SOD 44.36±2.82, and GPX 492.00±39.42, all P<0.001 vs. CCl_4). Similarly, in the CCl_4 + Y_2O_3 60 group, CAT 8.97±0.41, SOD 37.59±1.55, and GPX 322.75±17.50 were significantly higher than the CCl_4 group (P<0.001). CAT, SOD and GPX levels were remarkably higher in $Y_2O_3$60 group than those of the vehicle (16.00±0.53, 16.92±0.60 vs. 306.25±5.32 vs. 8.65±0.31, 10.50±0.40, 192.00±6.97; P<0.001). There were no significant differences between control and vehicle groups in CAT, SOD, and MDA values, whereas GPX was slightly lower in the vehicle group (192.00±13.95 vs 281.75±9.17; P<0.001) (figure 2B). Rat serum values for CAT, SOD, and MDA ratio showed no differences between vehicle and control group (8.65±0.31, 10.50±0.40, 0.99±0.59 vs. 10.5±0.39, 14.01±0.24, 0.66±0.21) (figures 2A, C, and D), Malondialdehyde (MDA), the lipid peroxidation marker, was significantly reduced by nanoparticle treatment (0.32±0.02 and 0.49±0.06 vs. CCl_4 0.70±0.05; P<0.001).

Serum Biochemical Analysis of (ALT, AST, ALP, and GGT) in Different Experimental Groups

Serum enzyme activities reflected hepatocellular damage induced by CCl_4. ALT, AST, and ALP increased significantly in the CCl_4 group compared with control animals (ALT 93.00±2.54 vs. 65.75±2.83; AST 286.33±2.89 vs. 166.50±10.15; ALP 645.00±16.62 vs. 392.75±23.43; P=0.001, P<0.001, P<0.001, respectively). (figure 2A-C). There were no significant differences in ALT levels between $Y_2O_3$45+CCl_4 and $Y_2O_3$60+CCl_4 groups compared with CCl_4 group (86.33±4.51 and 75.75±4.85 vs. 93.00±2.54, respectively).

Co-administration of Y_2O_3 nanoparticles remarkably improved these levels. ALT was reduced to (50.00±5.68 and 56.00±1.52 in $Y_2O_3$45 and $Y_2O_3$60 groups as compared to CCl_4+$Y_2O_3$45 group 86.33±4.51; P<0.001). AST also declined in $Y_2O_3$45+CCl_4 and $Y_2O_3$60+CCl_4 groups compared with CCl_4 group (154.66±9.00 and 178.00±7.35 vs 286.33±2.89; P<0.001).

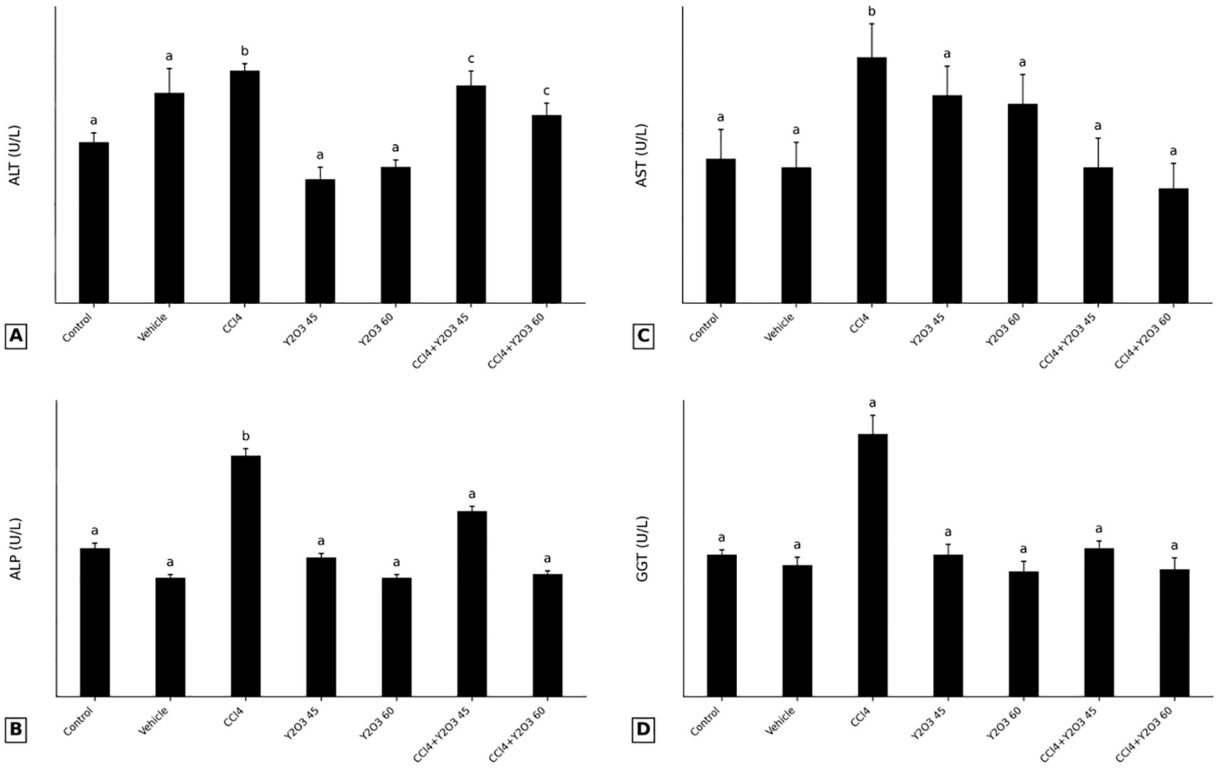

Figure 2: Serum biochemical analysis of liver injury markers in different experimental groups. Serum activities of liver injury markers were measured, including: (A) alanine aminotransferase (ALT), (B) alkaline phosphatase (ALP), (C) aspartate aminotransferase (AST), and (D) gamma-glutamyl transferase (GGT) activities. CCl_4 administration caused a significant increase in all measured liver enzymes compared with the control group, indicating hepatic injury and functional impairment. Treatment with Y_2O_3 nanoparticles at 45 and 60 mg/Kg significantly reduced the elevated enzyme activities in CCl_4-treated rats, with the higher dose showing a greater protective effect. Y_2O_3 nanoparticles alone did not significantly affect serum enzyme levels in healthy rats. Values are presented as mean±SD. Different letters indicate significant differences among groups (P<0.05).
Control (healthy rats), Vehicle (healthy rats treated with K_3PO_4), CCl_4 (healthy rats treated with CCl_4 to induce fibrosis), CCl_4+$Y_2O_3$45 (fibrotic rats treated with 45 mg/Kg Y_2O_3 NPs), CCl_4+$Y_2O_3$60 (fibrotic rats treated with 60 mg/Kg Y_2O_3 NPs), $Y_2O_3$45 (healthy rats treated with 45 mg/Kg Y_2O_3 NPs), $Y_2O_3$60 (healthy rats treated with 60 mg/Kg Y_2O_3 NPs).
ALT: Alanine aminotransferase; ALP: Alkaline phosphatase; AST: Aspartate aminotransferase; GGT: Gamma-glutamyl transferase; Y_2O_3 NPs: Yttrium oxide nanoparticles; CCl_4: Carbon tetrachloride; K_3PO_4: Potassium phosphate

In CCl_4+$Y_2O_3$60 group, ALT level was not significantly differences than that of $Y_2O_3$60 group (75.75±4.85 vs. 56.00±1.08; respectively) (figure 2A). CCl_4+$Y_2O_3$45 and CCl_4+$Y_2O_3$60 groups improved liver injury and decreased the elevation of AST and ALP compared with CCl_4 group (154.66±9.00, 497.66±9.87 and 178.00±7.35, 321.75±20.03 vs. 286.33±2.89, 645.00±16.62, P<0.001) (figures 2B and C). CCl_4+$Y_2O_3$60 groups showed a significant AST decrease as compared to $Y_2O_3$45 group (133.00±38.06 vs. 241.00±7.09; P<0.001, respectively) (figure 2C). In the present study, $Y_2O_3$60 and CCl_4+$Y_2O_3$60 groups significantly decreased the activity of ALP compared CCl_4+$Y_2O_3$45 groups (311.00±17.52 and 321.75±20.03 vs. 497.66±13.96; P<0.001, respectively) (figure 2B). Increase in the levels of GGT was observed in rats exposed to CCl_4 compared with the control, vehicle, $Y_2O_3$45, $Y_2O_3$60, CCl_4+$Y_2O_3$45 and CCl_4+$Y_2O_3$60 groups (619.00±33.17 vs. 337.75±32.58, 311.00±43.00, 349.66±42.36, 299.25±25.41, 344.00±26.31, and 294.33±24.25; P<0.001, respectively) (figure 2D). Data presented no significant differences in ALT, AST, ALP, and GGT between control and vehicle groups (65.75± 2.83, 166.50±10.15, 392.75±23.43, and 337.75±32.58 vs. 83.50±11.50, 155.00±20.00, 315.50±11.50, and 311.00±43.00, respectively) (figures 2A-D). There were no appreciable changes in ALT, AST and ALP in $Y_2O_3$45 and $Y_2O_3$60 rats relative to control (50.00±5.68, 241.00±7.09, 370.66±18.88, and 56.00±1.52, 232.33±9.83, 311.00±17.52 vs. 65.75±2.83, 65.75±2.83, and 392.75±23.43, respectively) (figure 2A-C). ALP showed a strong improvement (497.66±9.87 and 321.75±20.03 vs. 645.00±23.51; P< 0.001). Gamma-glutamyl transferase (GGT) activity was high in CCl_4-treated rats (619.00±33.17) but markedly attenuated in both nanoparticle-treated groups (344.00±26.31 and 294.33±24.25; P< 0.001). No significant differences were found between control and vehicle values.

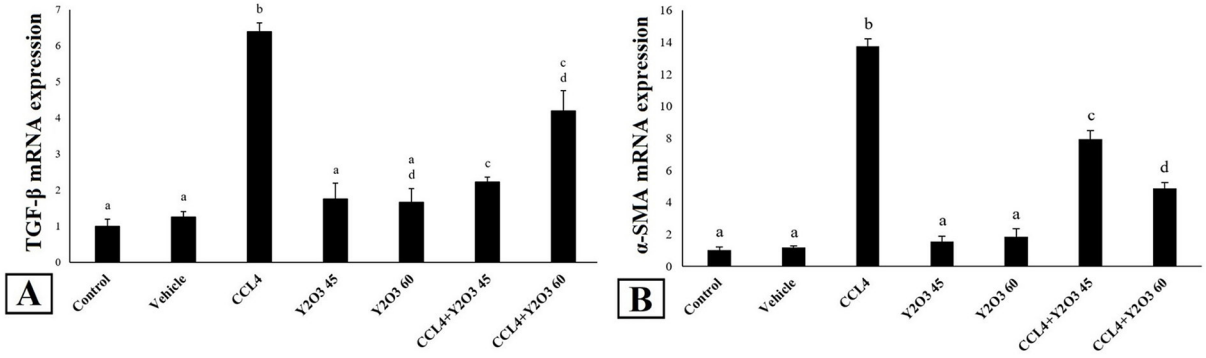

Figure 3: Hepatic mRNA expression of fibrogenic genes in different experimental groups. This figure illustrates the mRNA expression levels of (A) Transforming growth factor-beta (TGF-β) and (B) Alpha-smooth muscle actin (α-SMA) in different experimental groups. Gene expression was quantified by real-time PCR and normalized to the internal control gene GAPDH. Data are presented as mean±SE (n=8 per group). CCl_4 administration significantly upregulated the mRNA expression of both TGF-β and α-SMA compared to the control and vehicle groups (P<0.001). Co-treatment with Y_2O_3 nanoparticles at doses of 45 and 60 mg/Kg significantly downregulated the expression of these fibrogenic genes, indicating an attenuation of the fibrotic response. Bars sharing the same letter are not significantly different (P<0.05), while bars with different letters indicate significant differences (P<0.05).
Control (healthy rats), Vehicle (healthy rats treated with K_3PO_4), CCl_4 (healthy rats treated with CCl_4 to induce fibrosis), CCl_4+Y_2O_3 45 (fibrotic rats treated with 45 mg/Kg Y_2O_3 NPs), CCl_4+$Y_2O_3$60 (fibrotic rats treated with 60 mg/Kg Y_2O_3 NPs), $Y_2O_3$45 (healthy rats treated with 45 mg/Kg Y_2O_3 NPs), Y_2O_3 60 (healthy rats treated with 60 mg/Kg Y_2O_3 NPs).
TGF-β: Transforming growth factor beta; α-SMA: Alpha-smooth muscle actin; GAPDH: Glyceraldehyde-3-phosphate dehydrogenase; Y_2O_3 NPs: Yttrium oxide nanoparticles; CCl_4: Carbon tetrachloride; K_3PO_4: Potassium phosphate

Analysis of Hepatic TGF-β and α-SMA mRNA Expression

TGF-β and α-SMA evaluation followed by a statistical analysis indicated that there were no notable differences between the control and vehicle groups (1.00±0.20, 1.00±0.20, vs. 1.26±0.15, 1.17±0.09; respectively) (figure 3A and B). CCl_4 group induced the increase of TGF-β and α-SMA expression in contrast of the control and vehicle groups (6.40±0.23, 13.77±0.44 vs. 1.00±0.20, 1.00±0.20, and 1.17±0.98, 1.26±0.15; P<0.001; respectively) (figures 3A and B). The result showed that the expression of TGF-β and α-SMA had no significant difference in both $Y_2O_3$45 and $Y_2O_3$60 groups as compared with control and vehicle groups (1.76±0.43, 1.55±0.31 and 1.66±0.38, 1.86±0.49 vs. 1.00±0.20, 1.00±0.20 and 1.26±0.15, 1.17±0.98; respectively) (figures 3A and B). Although TGF-β and α-SMA expression is increased in CCl_4 group, but these increases were obviously decreased in CCl_4+$Y_2O_3$45 and CCl_4+$Y_2O_3$60 groups (6.40±0.23 (CCl_4) to 4.19±0.55, P=0.012 and 2.70±0.46, P=0.009, 13.77±0.44 (CCl_4) to7.94±0.54, P=0.002 and, 4.87±0.35, P=0.033) (figures 3A and B).

Hematoxylin and Eosin (H&E) and Masson's Trichrome (MTC) Staining Analysis

In this experiment, we used both H&E and MTC staining. An expert pathologist, blinded to the experiment, performed the histopathological evaluations to determine the hepatic injuries. Histological analysis was performed the liver of control and vehicle groups showed a normal tissue with a portal vein, central vein, sinusoids, and hepatocytes (figure 4A-P). Our findings showed extreme lipid vacuole accumulation (empty spaces in the figure), cellular ballooning, and lobar inflammation in CCl_4 group mice (figures 4C-Q). However, steatosis, edema, and inflammatory cells (Kupfer cells) were decreased in the CCl_4+$Y_2O_3$45 and 60 groups (figure 4F-U). A normal liver tissues were also observed in the $Y_2O_3$45 and 60 groups, only very small quantity of steatosis was observed in the 60 group (figures 4D-S).

In the first and second rows (H&E staining), the Control and Vehicle groups exhibit normal hepatic architecture with intact hepatocytes, clearly defined central veins (CV), portal veins (PV), and preserved sinusoidal spaces (yellow arrows). Hepatocyte nuclei are distinctly visible (yellow arrowheads). In contrast, the CCl_4-treated group shows severe histopathological alterations characterized by extensive macrovesicular and microvesicular steatosis (red arrowheads indicating lipid vacuoles), hepatocellular ballooning, marked lobular inflammation, and increased numbers of Kupffer cells (black arrows). Treatment with Y_2O_3 nanoparticles at 45 mg/Kg markedly improves liver histology, as evidenced by reduced steatosis, decreased inflammatory cell infiltration, and restoration of near-normal hepatocyte morphology. The CCl_4+$Y_2O_3$60 mg/Kg group demonstrates moderate amelioration of histopathological changes, although mild steatosis and occasional inflammatory foci persist.

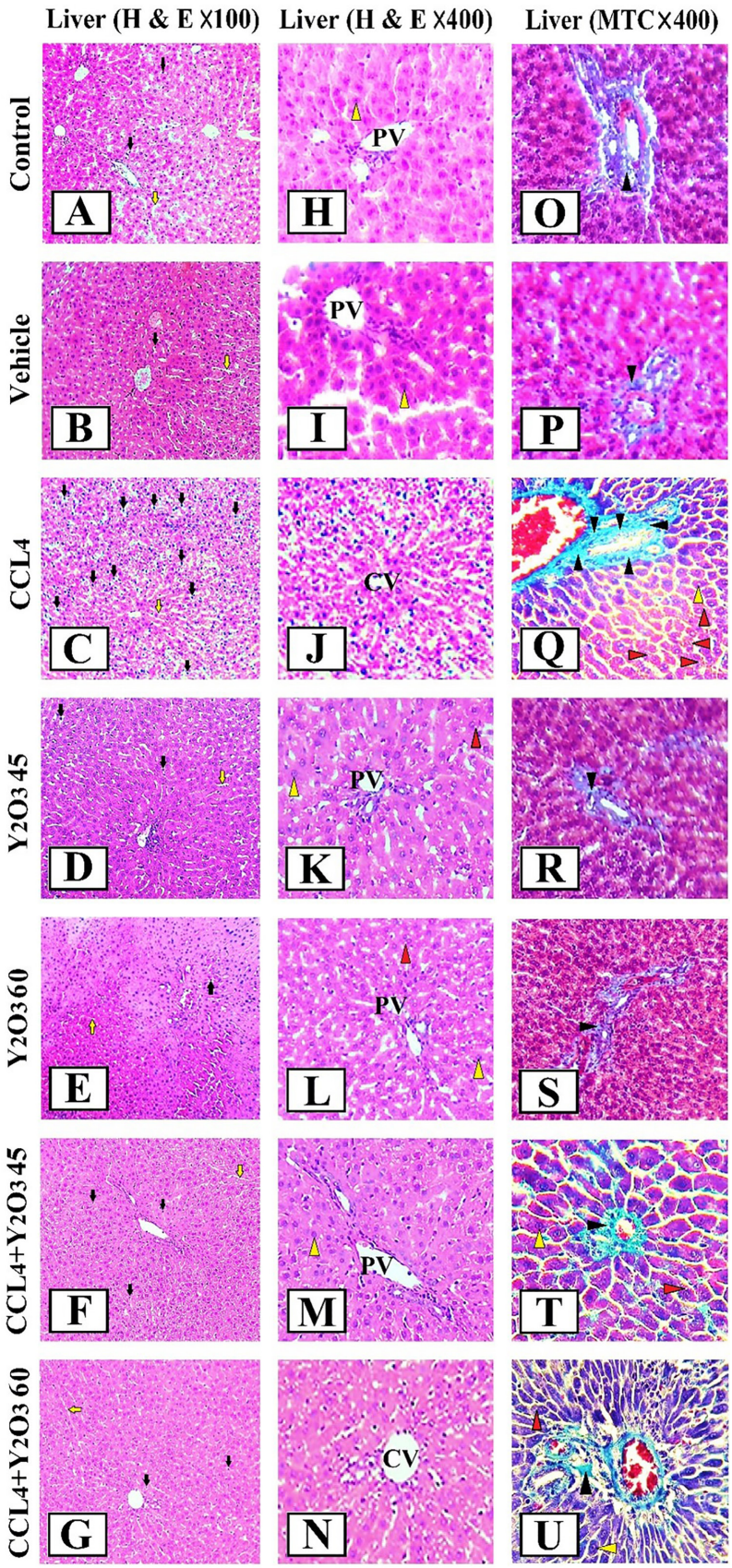

Figure 4: Histopathological evaluation of liver tissues in different experimental groups using Hematoxylin and Eosin (H&E) and Masson's Trichrome (MTC) staining. Representative photomicrographs are shown at ×100 and ×400 magnification.
H&E: Hematoxylin and eosin; MTC: Masson's trichrome; PV: Portal vein; CV: Central vein; Y_2O_3 NPs: Yttrium oxide nanoparticles; CCl_4: Carbon tetrachloride; K_3PO_4: Potassium phosphate.

The Y_2O_3 45 and 60 mg/Kg groups show liver architecture comparable to the Control group, with only minimal steatosis observed in the 60 mg/Kg group. In the third and fourth rows (MTC staining), the Control and Vehicle groups display minimal collagen deposition (light blue staining), confined mainly to vascular walls. The CCl_4 group exhibits extensive collagen fiber accumulation (light blue) in periportal and pericentral regions, indicating established liver fibrosis. Both CCl□+Y□O□ treatment groups show a significant reduction in collagen deposition compared to the CCl□ group, with the 45 mg/Kg dose demonstrating a more pronounced antifibrotic effect. The Y□O□-only groups show no abnormal collagen accumulation, confirming the biocompatibility of Y□O□ nanoparticles at the tested doses. Scale bars represent [insert value, e.g., 100 μm].

Discussion

The present study demonstrated, for the first time, that treatment with yttrium oxide nanoparticles (Y_2O_3 NPs) at doses of 45 and 60 mg/Kg significantly attenuated CCl_4-induced liver fibrosis in male Wistar rats. The liver, as a vital organ responsible for detoxification and metabolism,[1, 2] is susceptible to chronic injury leading to fibrosis.[3] Liver fibrosis results from persistent wound-healing response to damage[4] and can progress to cirrhosis and hepatocellular carcinoma.[5, 6] The hepatoprotective effects observed in this study were evidenced by enhanced antioxidant enzyme activities (CAT, SOD, GPX), reduced lipid peroxidation (MDA), decreased serum liver enzymes (AST, ALP, GGT), downregulation of fibrogenic genes (*TGF-β* and *α-SMA*), and improved histopathological features including reduced inflammation, steatosis, and collagen deposition. To the best of the authors' knowledge, this study is the first to report the treatment effects of Y_2O_3 NPs on liver fibrosis in Wistar rats. To date, many *in vivo* and *in vitro* studies have reported the biological effects of Y_2O_3 NPs, including anti-oxidant,[26] anti-inflammatory,[27] antibacterial,[29] and reduction of oxidative stress.[30]

CAT, SOD and GPX are the critical representative elements of endogenous antioxidant systems that mainly participate in the scavenging of free radicals.[31] In this study, a substantial decrease in the activity of CAT, SOD, and GPX was noted in the CCl_4-model of liver fibrosis in rats; thus suggesting harmful metabolic liver injury.[31] The study revealed the therapeutic effects of Y_2O_3 NPs against CCl_4-induced liver fibrosis by significantly increasing CAT, SOD, and GPX activity. Moreover, CAT, SOD, and GPX remarkable incretion by the administration of 60 mg/Kg Y_2O_3 NPs in non-fibrotic rats, were confirmed its potential regenerating biological antioxidant.[26]

In the same context, Kassem and others. demonstrated the potent antioxidant activity of Y_2O_3 NPs against hydroxyl and oxygen radicals as well as reduction in hydrogen peroxide concentration, rescuing the ROS damage effect and decrease in MDA concentration in environmentally stressed groups.[26] Our study revealed a significant increase in MDA concentration by CCl_4 administration in rats. Considerable evidence suggests that CCl_4 administration caused high levels of liver oxidative damage, significant elevation of ROS production and MDA concentration in the liver. [31] Moreover, our results showed that serum MDA level changes were significantly reduced upon treatment with Y_2O_3 NPs in CCl_4 rats.

Hepatic hypertrophy and toxicity are biologically responsible to the ALT, ALP, and AST liver enzymes increase.[32] In the current *in vivo* study, transaminases and transferase increasing directly linked with liver fibrosis caused by administration of CCl_4. Increase in biochemical enzymes indicated the potential of CCl_4 after injection to induce liver fibrosis.[32, 33]

Recent study reported that Y_2O_3 NPs decreased the liver enzymes towards normalization; indicating its liver protective effects as a free radical scavenger, antioxidant, and anti-apoptotic.[34] This demotion of enzymes activities would reverse hepatocyte damage, fibrosis and inflammatory reactions.[35] Our results demonstrated that serum ALP, AST and GGT enzymes decreased significantly in both CCl_4+Y_2O_3 groups. We also did not find any significant changes in ALT, ALP and GGT level between the control and Y_2O_3 NPs groups. These results confirmed Y_2O_3 nanoparticle nontoxic and rescue cell effects that has been reported earlier.[34]

A growing body of evidence indicates that TGF-β1/SMAD3 signaling mediates fibrogenesis in CCl_4 rat model.[36] Our findings demonstrated that CCl_4-induced liver fibrosis highlighting by the significant increase in TGF-β and α-SMA expression. Interestingly, repeated Y_2O_3 NPs administration (45 and 60 mg/Kg) significantly decreased the TGF-β and α-SMA expression indicating inhibition of hepatic fibrosis in CCl_4 rats.

Since the CCl_4-induced liver fibrosis ameliorates via suppressing the TGF-β/Smad3 signaling.[37] And on the other hand, Y_2O_3 NPs are cytocompatible, antioxidant and

anti-inflammator, also alleviate oxidative stress, inflammatory response, and subsequently liver injury.[38] These findings imply that probably Y_2O_3 NP_S administration could be used for modulating TGF-β and α-SMA overexpression in liver fibrosis. Our findings also revealed that TGF-β and α-SMA expression in non-fibrotic rats after 45 and 60 µg/Kg of Y_2O_3 NPs administration were similar to control group; which further confirmed antioxidant activity.[39]

Inflammation plays a critical role in hepatic pathology and failure, and chronic inflammation in the liver can lead to fibrosis, cirrhosis, and potentially cancer. Chronic liver inflammation is a primary driver of fibrosis, which can eventually lead to cirrhosis and hepatocellular carcinoma. Persistent injury activates Kupffer cells and hepatic stellate cells, initiating a cascade of fibrogenic responses that promote liver tissue damage.[40] Actually, the excessive accumulation of lipid in the liver leads to the activation of Kupffer and stellate cells,[39] and the release of cytokines and chemokines from them, finally inflammation and fibrosis in the liver.[41] Song and others have proved that Y_2O_3 NPs represented anti-inflammatory activity by inhibiting cellular reactive oxygen species-mediated NF-κB activation in vitro. A single intraperitoneal administration of Y_2O_3 NPs (30 mg/Kg) improved antioxidant status, reduced oxidative stress, inflammatory response, cell apoptosis, and liver damage in rats with fulminant hepatic failure.[23] In contrast to the above study, Panyala and others reported that oral administration of Y_2O_3 NPs (480 mg/Kg) for 28 days caused multifocal centrilobular necrosis with infiltration of inflammatory cells in liver tissue.[42] Findings of this study showed that treatment with Y_2O_3 NPs (45 and 60 mg/Kg) decreased inflammation, steatosis, cell edema, and collagen deposition, also the general structure of the liver was significantly normalized. However, analysis of the liver tissue shows that the rats receiving the Y_2O_3 NPs (45 mg/kg) had a better treatment. Based on mentioned points, Y_2O_3 NPs in higher doses seem to have less therapeutic effects and even cause injury in the liver tissue.

The superior efficacy of the 45 mg/kg dose compared to 60 mg/Kg in several parameters, including antioxidant enzyme activities and histopathological scores, suggests a non-linear dose-response relationship. This phenomenon may be explained by the hormesis concept, where low doses stimulate beneficial biological responses while higher doses become inhibitory or toxic. This biphasic response has been previously documented for various nanoparticles and warrants further investigation to establish the optimal therapeutic window for Y_2O_3 NPs in liver fibrosis. This discrepancy highlights the importance of dose in determining the biological effects of nanoparticles. The doses used in our study (45 and 60 mg/Kg, intraperitoneal) were substantially lower and demonstrated therapeutic effects without evident toxicity, as confirmed by normal liver histology in healthy rats treated with Y_2O_3 NPs alone. This suggests that Y_2O_3 NPs exhibit a narrow therapeutic window, where low to moderate doses confer hepatoprotection, while high doses may induce toxicity. Similar dose-dependent effects have been reported for other metal oxide nanoparticles.[34]

Despite the promising findings, this study has several limitations that should be acknowledged. First, the study duration was limited to 4 weeks, and longer-term studies are needed to assess the sustainability of the therapeutic effects and potential chronic toxicity. Second, while we demonstrated downregulation of TGF-β and α-SMA, the precise molecular mechanisms particularly the involvement of the Smad-dependent pathway is not elucidated. Third, only two doses were tested, limiting our ability to fully characterize the dose-response relationship. Fourth, the biodistribution, pharmacokinetics, and long-term fate of Y_2O_3 NPs in the body were not assessed.

Conclusion

In conclusion, this study provides the first evidence that Y_2O_3 NPs at doses of 45 and 60 mg/Kg effectively attenuate CCl_4-induced liver fibrosis in rats through multiple mechanisms: enhancement of antioxidant defense systems, reduction of oxidative stress, normalization of liver enzymes, downregulation of fibrogenic gene expression, and improvement of histopathological features. The 45 mg/Kg dose demonstrated superior efficacy in several parameters, suggesting a non-linear dose-response relationship. These findings position Y_2O_3 NPs as promising candidates for liver fibrosis therapy, though further studies are warranted to establish the optimal dosing regimen, elucidate precise molecular mechanisms, and evaluate long-term safety and efficacy before clinical translation can be considered.

Acknowledgment

We wish to express our sincere gratitude to all individuals and institutions whose contributions were vital to the success of this study. This research was extracted from the PhD thesis of Fatemeh Daneshpazhooh. We would like to

thank the laboratory of Islamic Azad University, Qom Branch, for providing us with the necessary facilities to conduct this research.

Authors' Contribution

F.D: Conceptualization, study design, acquisition, analysis, and interpretation of data for the work; drafting the work; Sh.O: Conceptualization, study design, analysis and interpretation of data for the work, and reviewing the manuscript; P.M: Study design, data interpretation, and reviewing the manuscript; All authors have read and approved the final manuscript and agree to be accountable for all aspects of the work in ensuring that questions related to the accuracy or integrity of any part of the work are appropriately investigated and resolved.

Declaration of AI

No artificial intelligence tools were used in the preparation of this manuscript.

Conflict of Interest: None declared.

References

1 Kalra A, Yetiskul E, Wehrle CJ, Tuma F. Physiology, liver. In: StatPearls [Internet]. Treasure Island (FL): StatPearls Publishing; 2022 [cited 2026 Feb 18]. Available from: https://www.statpearls.com/articlelibrary/viewarticle/36037

2 Ehrlich A, Duche D, Ouedraogo G, Nahmias Y. Challenges and Opportunities in the Design of Liver-on-Chip Microdevices. Annu Rev Biomed Eng. 2019;21:219-39. doi: 10.1146/annurev-bioeng-060418-052305. PubMed PMID: 31167098; PubMed Central PMCID: PMC7004816.

3 Acharya P, Chouhan K, Weiskirchen S, Weiskirchen R. Cellular Mechanisms of Liver Fibrosis. Front Pharmacol. 2021;12:671640. doi: 10.3389/fphar.2021.671640. PubMed PMID: 34025430; PubMed Central PMCID: PMC8134740.

4 Nan Y, Su H, Lian X, Wu J, Liu S, Chen P, et al. Pathogenesis of Liver Fibrosis and Its TCM Therapeutic Perspectives. Evid Based Complement Alternat Med. 2022;2022:5325431. doi: 10.1155/2022/5325431. PubMed PMID: 35529927; PubMed Central PMCID: PMC9071861.

5 Dhar D, Baglieri J, Kisseleva T, Brenner DA. Mechanisms of liver fibrosis and its role in liver cancer. Exp Biol Med (Maywood). 2020;245:96-108. doi: 10.1177/1535370219898141. PubMed PMID: 31924111; PubMed Central PMCID: PMC7016420.

6 Yilma M, Saxena V, Mehta N. Models to Predict Development or Recurence of Hepatocellular Carcinoma (HCC) in Patients with Advanced Hepatic Fibrosis. Curr Gastroenterol Rep. 2022;24:1-9. doi: 10.1007/s11894-022-00835-8. PubMed PMID: 35142988; PubMed Central PMCID: PMC8891098.

7 Li X, Zhang Q, Wang Z, Zhuang Q, Zhao M. Immune and Metabolic Alterations in Liver Fibrosis: A Disruption of Oxygen Homeostasis? Front Mol Biosci. 2021;8:802251. doi: 10.3389/fmolb.2021.802251. PubMed PMID: 35187072; PubMed Central PMCID: PMC8850363.

8 Frangogiannis N. Transforming growth factor-beta in tissue fibrosis. J Exp Med. 2020;217:e20190103. doi: 10.1084/jem.20190103. PubMed PMID: 32997468; PubMed Central PMCID: PMC7062524.

9 Gupta P, Sata TN, Yadav AK, Mishra A, Vats N, Hossain MM, et al. TGF-beta induces liver fibrosis via miRNA-181a-mediated down regulation of augmenter of liver regeneration in hepatic stellate cells. PLoS One. 2019;14:e0214534. doi: 10.1371/journal.pone.0214534. PubMed PMID: 31166951; PubMed Central PMCID: PMC6550375.

10 Komolkriengkrai M, Nopparat J, Vongvatcharanon U, Anupunpisit V, Khimmaktong W. Effect of glabridin on collagen deposition in liver and amelioration of hepatocyte destruction in diabetes rats. Exp Ther Med. 2019;18:1164-74. doi: 10.3892/etm.2019.7664. PubMed PMID: 31316610; PubMed Central PMCID: PMC6601403.

11 Tian F, Liu Y, Gao J, Yang N, Shang X, Lv J, et al. Study on the association between TGF-beta1 and liver fibrosis in patients with hepatic cystic echinococcosis. Exp Ther Med. 2020;19:1275-80. doi: 10.3892/etm.2019.8355. PubMed PMID: 32010299; PubMed Central PMCID: PMC6966196.

12 Gu L, Zhang F, Wu J, Zhuge Y. Nanotechnology in Drug Delivery for Liver Fibrosis. Front Mol Biosci. 2021;8:804396. doi: 10.3389/fmolb.2021.804396. PubMed PMID: 35087870; PubMed Central PMCID: PMC8787125.

13 Yadav PK, Saklani R, Tiwari AK, Verma S, Rana R, Chauhan D, et al. Enhanced apoptosis and mitochondrial cell death by paclitaxel-loaded TPP-TPGS(1000)-functionalized nanoemulsion. Nanomedicine (Lond). 2023;18:343-66. doi: 10.2217/nnm-2022-0268. PubMed PMID: 37140535.

14 Su S, P MK. Recent Advances in Nanocarrier-Assisted Therapeutics Delivery Systems. Pharmaceutics. 2020;12. doi: 10.3390/pharmaceutics12090837. PubMed PMID: 32882875; PubMed Central PMCID: PMC7559885.
15 Zhang P, Xia J, Luo S. Generation of Well-Defined Micro/Nanoparticles via Advanced Manufacturing Techniques for Therapeutic Delivery. Materials (Basel). 2018;11. doi: 10.3390/ma11040623. PubMed PMID: 29670013; PubMed Central PMCID: PMC5951507.
16 Huang C, Chen X, Xue Z, Wang T. Effect of structure: A new insight into nanoparticle assemblies from inanimate to animate. Sci Adv. 2020;6:1321. doi: 10.1126/sciadv.aba1321. PubMed PMID: 32426506; PubMed Central PMCID: PMC7220353.
17 Maslanka Figueroa S, Fleischmann D, Goepferich A. Biomedical nanoparticle design: What we can learn from viruses. J Control Release. 2021;329:552-69. doi: 10.1016/j.jconrel.2020.09.045. PubMed PMID: 33007365; PubMed Central PMCID: PMC7525328.
18 Fish MB, Banka AL, Braunreuther M, Fromen CA, Kelley WJ, Lee J, et al. Deformable microparticles for shuttling nanoparticles to the vascular wall. Sci Adv. 2021;7. doi: 10.1126/sciadv.abe0143. PubMed PMID: 33883129; PubMed Central PMCID: PMC8059934.
19 de la Torre P, Perez-Lorenzo MJ, Alcazar-Garrido A, Flores AI. Cell-Based Nanoparticles Delivery Systems for Targeted Cancer Therapy: Lessons from Anti-Angiogenesis Treatments. Molecules. 2020;25. doi: 10.3390/molecules25030715. PubMed PMID: 32046010; PubMed Central PMCID: PMC7038177.
20 Gomes HIO, Martins CSM, Prior JAV. Silver Nanoparticles as Carriers of Anticancer Drugs for Efficient Target Treatment of Cancer Cells. Nanomaterials (Basel). 2021;11. doi: 10.3390/nano11040964. PubMed PMID: 33918740; PubMed Central PMCID: PMC8069134.
21 Rajakumar G, Mao L, Bao T, Wen W, Wang S, Gomathi T, et al. Yttrium oxide nanoparticle synthesis: an overview of methods of preparation and biomedical applications. Appl Sci (Basel). 2021;11:2172. doi: 10.3390/app11052172.
22 Navaei-Nigjeh M, Daniali M, Rahimifard M, Khaksar MR. Multi-organ Toxicity Attenuation by Cerium Oxide and Yttrium Oxide Nanoparticles: Comparing the Beneficial Effects on Tissues Oxidative Damage Induced by Sub-acute Exposure to Diazinon. Pharm Nanotechnol. 2020;8:225-38. doi: 10.2174/2211738508666200808135226. PubMed PMID: 32767961.
23 Song X, Shang P, Sun Z, Lu M, You G, Yan S, et al. Therapeutic effect of yttrium oxide nanoparticles for the treatment of fulminant hepatic failure. Nanomedicine (Lond). 2019;14:2519-33. doi: 10.2217/nnm-2019-0154. PubMed PMID: 31317822.
24 Akhtar MJ, Ahamed M, Alrokayan SA, Ramamoorthy MM, Alaizeri ZM. High Surface Reactivity and Biocompatibility of Y(2)O(3) NPs in Human MCF-7 Epithelial and HT-1080 FibroBlast Cells. Molecules. 2020;25. doi: 10.3390/molecules25051137. PubMed PMID: 32138335; PubMed Central PMCID: PMC7179248.
25 Charles River Laboratories. Guide for the care and use of laboratory animals. Westborough: Charles River Laboratories; 2018.
26 Kassem S, Arafa MM, Yehya MM, Soliman MAM. In vivo study of dose-dependent antioxidant efficacy of functionalized core-shell yttrium oxide nanoparticles. Naunyn Schmiedebergs Arch Pharmacol. 2022;395:593-606. doi: 10.1007/s00210-022-02219-1. PubMed PMID: 35201389; PubMed Central PMCID: PMC8989852.
27 Tang KS. Antioxidant and Anti-inflammatory Properties of Yttrium Oxide Nanoparticles: New Insights into Alleviating Diabetes. Curr Diabetes Rev. 2021;17:496-502. doi: 10.2174/1573399816999201012201111. PubMed PMID: 33045978.
28 Bancroft JD, Gamble M. Theory and practice of histological techniques. 8th ed. Amsterdam: Elsevier; 2019.
29 Akanbi TO, Ojo S, Adedayo BM, Olayanju O, Akinpelu O. Antibacterial properties of yttrium oxide nanoparticles against multidrug resistant bacteria. J Nanobiotechnology. 2021;19:123.
30 Mohamed HRH, Farouk AH, Elbasiouni SH, Nasif KA, Safwat G. Yttrium oxide nanoparticles ameliorates calcium hydroxide and calcium titanate nanoparticles induced genomic DNA and mitochondrial damage, ROS generation and inflammation. Sci Rep. 2024;14:13015. doi: 10.1038/s41598-024-62877-4. PubMed PMID: 38844752; PubMed Central PMCID: PMC11156978.
31 Wali AF, Ali S, Rashid S, Alsaffar RM, Arafah A, Qamar W, et al. Attenuation of oxidative damage-associated hepatotoxicity by piperine in CCl_4-induced liver fibrosis. J King Saud Univ Sci. 2021;33:101629. doi: 10.1016/j.jksus.2021.101629. doi: 10.1016/j.jksus.2021.101629.

32 Izzularab BM, Megeed M, Yehia M. Propolis nanoparticles modulate the inflammatory and apoptotic pathways in carbon tetrachloride-induced liver fibrosis and nephropathy in rats. Environ Toxicol. 2021;36:55-66. doi: 10.1002/tox.23010. PubMed PMID: 32840962.
33 Dutta S, Chakraborty AK, Dey P, Kar P, Guha P, Sen S, et al. Amelioration of CCl_4 induced liver injury in swiss albino mice by antioxidant rich leaf extract of Croton bonplandianus Baill. PLoS One. 2018;13:e0196411. doi: 10.1371/journal.pone.0196411. PubMed PMID: 29709010; PubMed Central PMCID: PMC5927454.
34 Abbasi E, Vafaei SA, Naseri N, Darini A, Azandaryani MT, Ara FK, et al. Protective effects of cerium oxide nanoparticles in non-alcoholic fatty liver disease (NAFLD) and carbon tetrachloride-induced liver damage in rats: Study on intestine and liver. Metabol Open. 2021;12:100151. doi: 10.1016/j.metop.2021.100151. PubMed PMID: 34870139; PubMed Central PMCID: PMC8626579.
35 Abdorrashidi M, Peypar MH, Tohidinia A, Zali F, Eisazadeh S, Abyazi MA, et al. Efforts Focused on Fatty Liver over Two Years (2023-2025): A Thematic Literature Review. Iran J Pathol. 2025;20:355-66. doi: 10.30699/ijp.2025.2047720.3391. PubMed PMID: 41099052; PubMed Central PMCID: PMC12520595.
36 Ogaly HA, Aldulmani SAA, Al-Zahrani FAM, Abd-Elsalam RM. D-Carvone Attenuates CCl(4)-Induced Liver Fibrosis in Rats by Inhibiting Oxidative Stress and TGF-ss 1/SMAD3 Signaling Pathway. Biology (Basel). 2022;11. doi: 10.3390/biology11050739. PubMed PMID: 35625467; PubMed Central PMCID: PMC9138456.
37 Wu S, Liu L, Yang S, Kuang G, Yin X, Wang Y, et al. Paeonol alleviates CCl(4)-induced liver fibrosis through suppression of hepatic stellate cells activation via inhibiting the TGF-beta/Smad3 signaling. Immunopharmacol Immunotoxicol. 2019;41:438-45. doi: 10.1080/08923973.2019.1613427. PubMed PMID: 31119954.
38 Ribera J, Rodriguez-Vita J, Cordoba B, Portoles I, Casals G, Casals E, et al. Functionalized cerium oxide nanoparticles mitigate the oxidative stress and pro-inflammatory activity associated to the portal vein endothelium of cirrhotic rats. PLoS One. 2019;14:e0218716. doi: 10.1371/journal.pone.0218716. PubMed PMID: 31233564; PubMed Central PMCID: PMC6590813.v
39 Feng S, Tong H, Gao JH, Tang SH, Yang WJ, Wang GM, et al. Anti-inflammation treatment for protection of hepatocytes and amelioration of hepatic fibrosis in rats. Exp Ther Med. 2021;22:1213. doi: 10.3892/etm.2021.10647. PubMed PMID: 34584558; PubMed Central PMCID: PMC8422404.
40 Tanwar S, Rhodes F, Srivastava A, Trembling PM, Rosenberg WM. Inflammation and fibrosis in chronic liver diseases including non-alcoholic fatty liver disease and hepatitis C. World J Gastroenterol. 2020;26:109-33. doi: 10.3748/wjg.v26.i2.109. PubMed PMID: 31969775; PubMed Central PMCID: PMC6962431.
41 Chen L, Zhang Q, Yu C, Wang F, Kong X. Functional roles of CCL5/RANTES in liver disease. Liver Res. 2020;4:28-34. doi: 10.1016/j.livres.2020.01.002. doi: 10.1016/j.livres.2020.01.002.
42 Panyala A, Chinde S, Kumari SI, Rahman MF, Mahboob M, Kumar JM, et al. Comparative study of toxicological assessment of yttrium oxide nano- and microparticles in Wistar rats after 28 days of repeated oral administration. Mutagenesis. 2019;34:181-201. doi: 10.1093/mutage/gey044. PubMed PMID: 30753658.